Journal of ELECTRONIC MATERIALS, Vol. 47, No. 6, 2018
https://doi.org/10.1007/s11664-017-5891-0

TOPICAL COLLECTION: INTERNATIONAL CONFERENCE ON THERMOELECTRICS 2017

Beneficial Effect of S-Filling on Thermoelectric Properties of $S_xCo_4Sb_{11.2}Te_{0.8}$ Skutterudite

HONGTAO WANG,[1] BO DUAN,[1,3] GUANGHUI BAI,[2] JIALIANG LI,[1] YUE YU,[1] HOUJIANG YANG,[1] GANG CHEN,[1] and PENGCHENG ZHAI[1,4]

1.—Hubei Key Laboratory of Theory and Application of Advanced Materials Mechanics, Wuhan University of Technology, Wuhan 430070, China. 2.—Science and Technology on Space Physics Laboratory, Beijing 100076, China. 3.—e-mail: duanboabc@126.com. 4.—e-mail: pczhai@126.com

In this work, Te-doped and S-filled $S_xCo_4Sb_{11.2}Te_{0.8}$ (x = 0.1, 0.15, 0.2, 0.25, 0.3, 0.4) skutterudite compounds have been prepared using solid state reaction and spark plasma sintering. Thermoelectric measurements of the consolidated samples were examined in a temperature range of 300–850 K, and the influences of S-addition on the thermoelectric properties of $S_xCo_4Sb_{11.2}Te_{0.8}$ skutterudites are systematically investigated. The results indicate that the addition of sulfur and tellurium is effective in reducing lattice thermal conductivity due to the point-defect scattering caused by tellurium substitutions and the cluster vibration brought by S-filling. The solubility of tellurium in skutterudites is enhanced with sulfur addition via charge compensation. The thermal conductivity decreases with increasing sulfur content. The highest figure of merit, ZT = 1.5, was obtained at 850 K for $S_{0.3}Co_4Sb_{11.2}Te_{0.8}$ sample, because of the low lattice thermal conductivity.

Key words: Skutterudite, S-filling, thermoelectric properties, charge compensation

INTRODUCTION

Thermoelectrics is a promising technology for converting waste heat directly into electricity and can be used for cooling and heating in electric vehicles with the advantages of quick operation, no greenhouse gas emissions and high reliability.[1–4] The efficiency of power generation of these thermoelectric materials is indexed by the dimensionless figure of merit, which is defined as $ZT = \alpha^2\sigma T/\kappa$, where α is the Seebeck coefficient, σ is the electrical conductivity, T is the absolute temperature, and κ is the thermal conductivity composed of electronic thermal conductivity κ_e and the lattice thermal conductivity κ_L.

$CoSb_3$-based skutterudite compounds have been attracting substantial interest because of their promising thermoelectric performance in the intermediate temperature range due to their excellent electrical transport properties and large Seebeck coefficient, but thermal conductivity of the binary skutterudites is too large for thermoelectric applications.[5] Decreasing the thermal conductivity and increasing the electric transport properties of thermoelectric materials are important directions of thermoelectric material researches.[6]

Various approaches have been taken to reduce the thermal conductivity and improve the thermoelectric performance of $CoSb_3$-based skutterudites, such as incorporating nanoparticles into the matrix to scatter high-frequency phonons,[7–9] substituting the antimony sites or cobalt sites with dopant atoms[10–17] to perturb the vibration of Sb_4-ring and enhance phonon scattering on impurities, and filling atoms into the voids of skutterudites[18–25] results in a manifestation of the Phonon Glass Electron Crystal (PGEC) concept, which can achieve good electrical transport properties and low thermal conductivity at the same time due to the presence of filler atoms in the skutterudite voids.[25] The Yb/Sr-filled and Ge/Sn-

(Received July 31, 2017; accepted October 23, 2017; published online November 9, 2017)

doped $CoSb_3$ skutterudites were synthesized, and their thermoelectric properties have been investigated.[26–28] The obtained results have demonstrated that doping with Ge/Sn in electropositive guest-filled skutterudite materials can increase Yb/Sr incorporation and is an effective method of enhancing the thermoelectric performance.[26–28]

Recently, the findings of electronegative filling in $CoSb_3$-based skutterudites provide a new perspective for guest-filling in skutterudites materials.[19,20,24] The results of electronegative filling indicated that introducing electronegative guests into skutterudite hollow structures influences the lattice dynamics and reduces lattice thermal conductivity significantly. In this study, the solid state reaction was attempted to prepare the S-filled and Te-doped skutterudite compounds. The influences of charge compensation between tellurium and sulfur have been studied. The tellurium doping fractions are successfully increased via charge compensation, leading to an excellent thermoelectric performance.

EXPERIMENTAL PROCEDURE

Te-doped and S-filled skutterudite compounds $S_xCo_4Sb_{11.2}Te_{0.8}$ (x = 0.1, 0.15, 0.2, 0.25, 0.3, 0.4) have been prepared using solid state reaction and spark plasma sintering (SPS). The powders of sulfur (purity 99.999%), cobalt (purity 99.9%), antimony (purity 99.999%), and tellurium (purity 99.999%) were blended in stoichiometric compositions and then loaded into the carbon crucible. The crucible was sealed under a vacuum, heated up slowly to 903 K and held for 72 h. The obtained materials were ground and sintered by SPS at 903 K for 7 min.

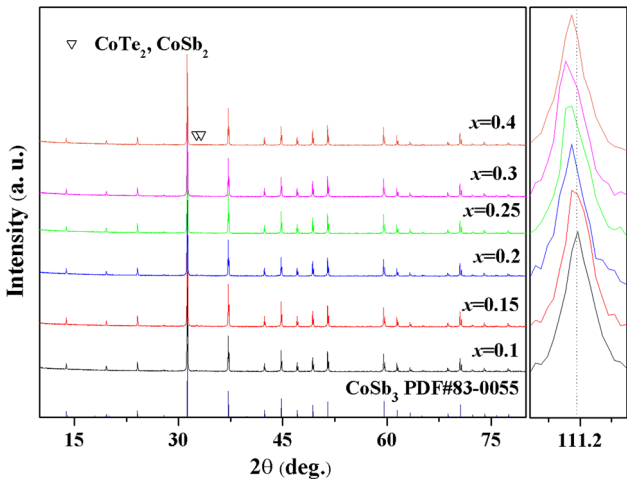

Fig. 1. XRD patterns obtained for $S_xCo_4Sb_{11.2}Te_{0.8}$ (x = 0.1, 0.15, 0.2, 0.25, 0.3, 0.4) compounds.

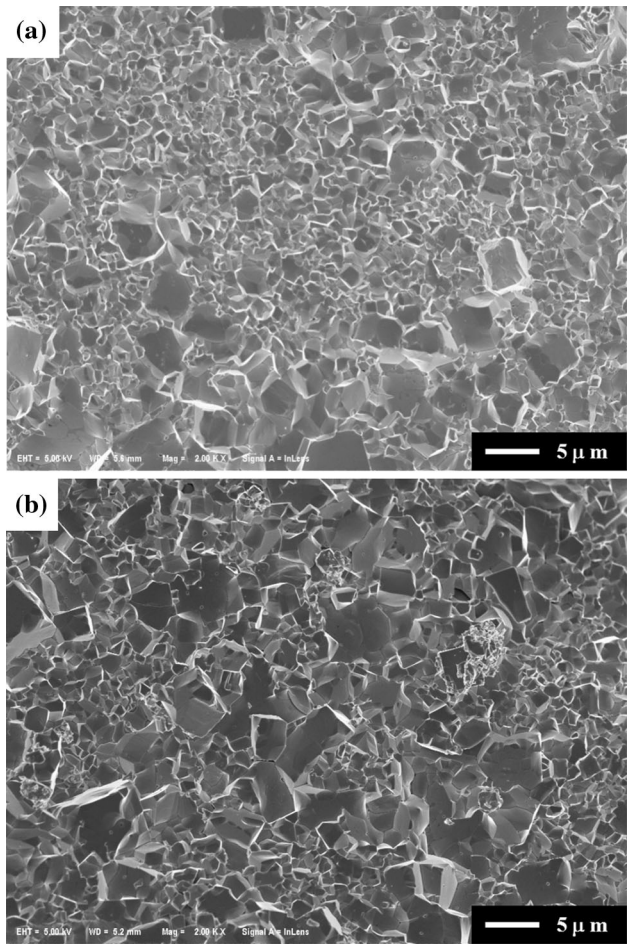

Fig. 2. FESEM images for $S_xCo_4Sb_{11.2}Te_{0.8}$ samples. (a) x = 0.1, (b) x = 0.3.

Table I. The nominal composition, actual composition (EPMA), lattice parameter α (Å) and density d (g cm^{-3}) for $S_xCo_4Sb_{11.2}Te_{0.8}$

Nominal composition	EPMA	α (Å)	d (g cm^{-3})
$S_{0.1}Co_4Sb_{11.2}Te_{0.8}$	$S_{0.12}Co_4Sb_{11.26}Te_{0.59}$	9.0506	7.54
$S_{0.15}Co_4Sb_{11.2}Te_{0.8}$	$S_{0.17}Co_4Sb_{11.22}Te_{0.66}$	9.0508	7.59
$S_{0.2}Co_4Sb_{11.2}Te_{0.8}$	$S_{0.22}Co_4Sb_{11.19}Te_{0.70}$	9.0513	7.60
$S_{0.25}Co_4Sb_{11.2}Te_{0.8}$	$S_{0.24}Co_4Sb_{11.16}Te_{0.73}$	9.0518	7.61
$S_{0.3}Co_4Sb_{11.2}Te_{0.8}$	$S_{0.26}Co_4Sb_{11.19}Te_{0.77}$	9.0520	7.55
$S_{0.4}Co_4Sb_{11.2}Te_{0.8}$	$S_{0.27}Co_4Sb_{11.12}Te_{0.75}$	9.0518	7.54

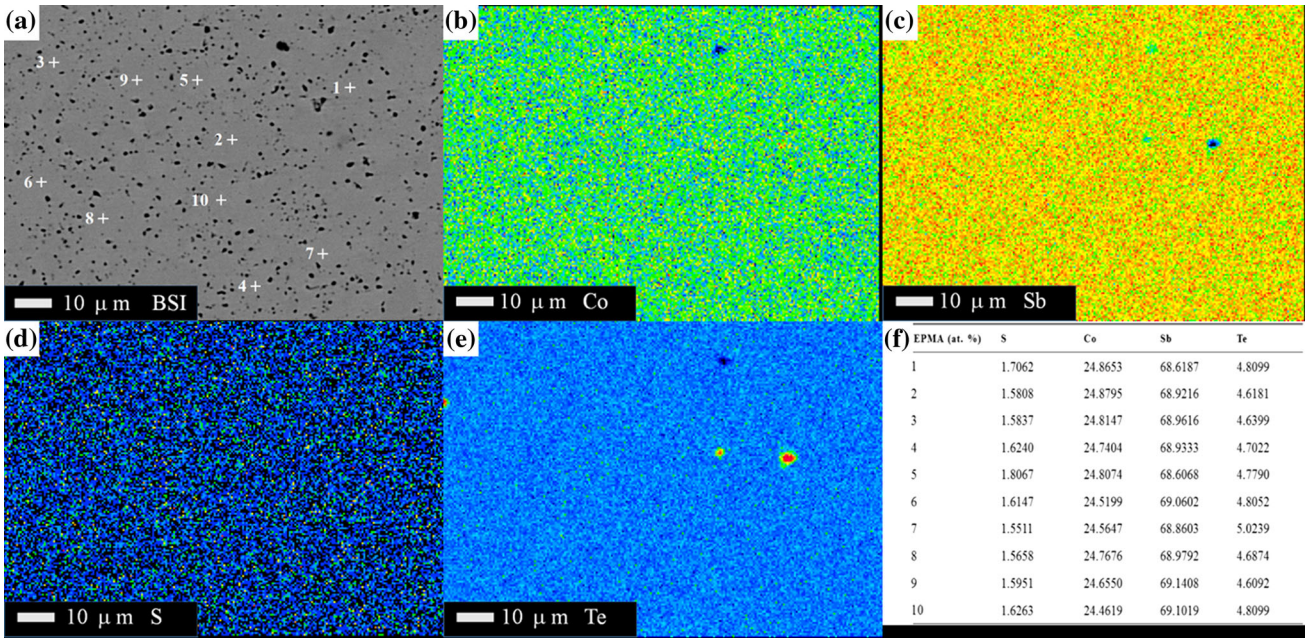

EPMA (at. %)	S	Co	Sb	Te
1	1.7062	24.8653	68.6187	4.8099
2	1.5808	24.8795	68.9216	4.6181
3	1.5837	24.8147	68.9616	4.6399
4	1.6240	24.7404	68.9333	4.7022
5	1.8067	24.8074	68.6068	4.7790
6	1.6147	24.5199	69.0602	4.8052
7	1.5511	24.5647	68.8603	5.0239
8	1.5658	24.7676	68.9792	4.6874
9	1.5951	24.6550	69.1408	4.6092
10	1.6263	24.4619	69.1019	4.8099

Fig. 3. The BSI (a), elemental mapping distribution (b–e) and point-compositions (f) of $S_{0.3}Co_4Sb_{11.2}Te_{0.8}$ sample.

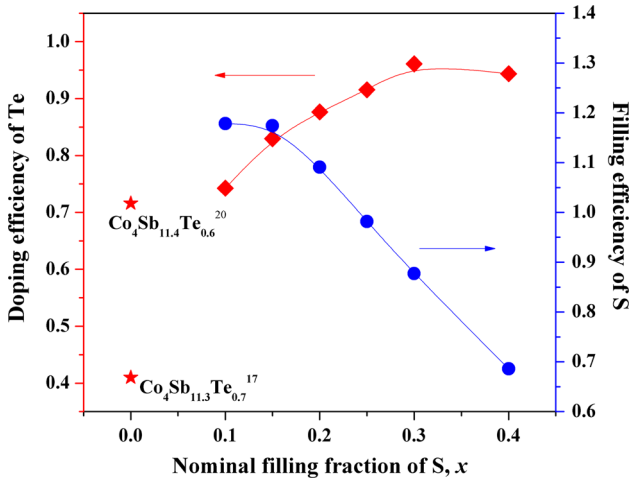

Fig. 4. The nominal S-filling fraction versus Te-doping efficiency and S-filling efficiency.

The skutterudite phase of the samples was verified by powder x-ray diffractometry (XRD, Bruker: D8 Advance, Cu Kα). The micro-structures of samples were characterized by using field emitting scanning electron microscopy (FESEM; Zeiss Ultra Plus). The back-scattered electron image (BSI) and the chemical composition of the polished surfaces were obtained with an electron probe micro-analyzer (EPMA; JXA-8230, Japan) equipped with wavelength dispersive x-ray spectroscope (WDS). The measurements of Seebeck coefficient and electrical conductivity were accomplished by standard four-probe method (ZEM-3; Sinku-riko) synchronously. Thermal diffusivity (λ) were measured using a laser-flash technique (Netzsch: LFA-457), and the heat capacity (C_p) was measured by the differential scanning calorimeter (TA: DSC Q20). The thermal conductivity was calculated by the formula $\kappa = C_p\lambda d$, where d was density of the materials.

RESULTS AND DISCUSSION

Figure 1 displays the XRD patterns of $S_xCo_4Sb_{11.2}Te_{0.8}$ (x = 0.1, 0.15, 0.2, 0.25, 0.3, 0.4) samples. As shown in Fig. 1, besides the main $CoSb_3$ phase, very small amounts of second phases, such as $CoTe_2$ and $CoSb_2$ were detected in $S_xCo_4Sb_{11.2}Te_{0.8}$ (x = 0.1, 0.15, 0.2) samples. As the doping fraction is equal or exceeding 0.25, the peaks of the impurity phases disappear. The right part of Fig. 1 shows local enlargement of the high-angle diffraction patterns for $S_xCo_4Sb_{11.2}Te_{0.8}$. The high-angle peaks of $S_xCo_4Sb_{11.2}Te_{0.8}$ ($x \le 0.3$) shift to lower angle with increasing filling fraction of sulfur, indicating lattice expansion due to the increased doping fraction of tellurium as shown in Table I (will be discussed later).

The samples' microstructures were analyzed by FESEM on the fractured surface of representative samples of $S_xCo_4Sb_{11.2}Te_{0.8}$ (x = 0.1, 0.3), as shown in Fig. 2. The matrix is densely compacted, which is in agreement with the high density values as shown in Table I. The grains of these samples are smaller and uniform than single Te-doped skutterudite.[17] For $S_{0.1}Co_4Sb_{11.2}Te_{0.8}$, the sizes of most particles are within the range of 1–5 μm, as shown in Fig. 2a. Figure 2b shows the microstructure of sample $S_{0.3}Co_4Sb_{11.2}Te_{0.8}$, and there is a certain increase in the amount of particles that are larger than 5 μm, compared to $S_{0.1}Co_4Sb_{11.2}Te_{0.8}$. The grain growth of

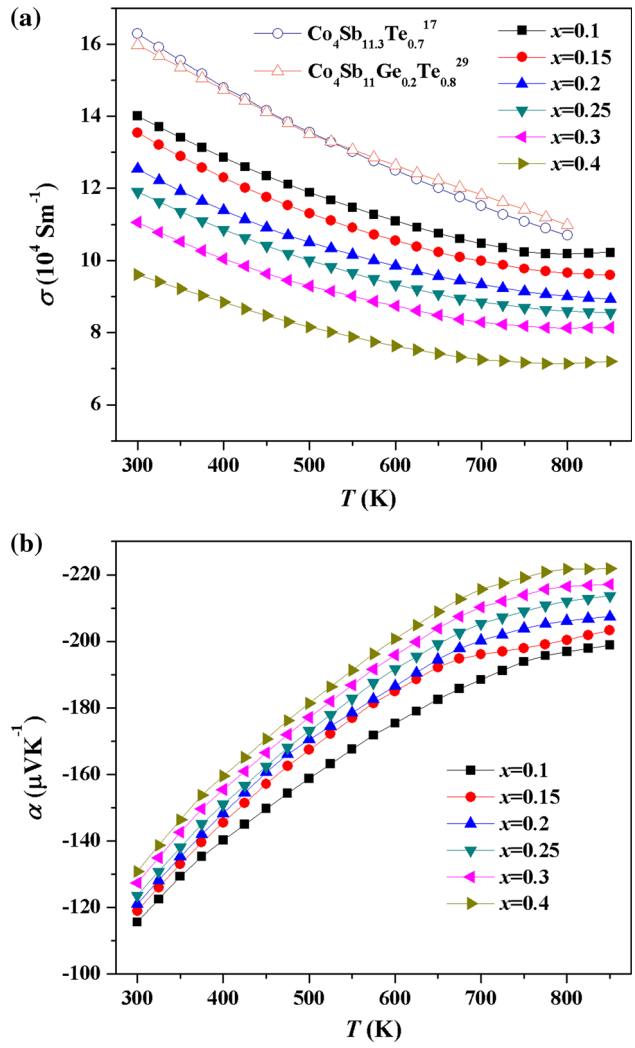

Fig. 5. Temperature dependence of electrical conductivity (a) and Seebeck coefficient (b) for all samples.

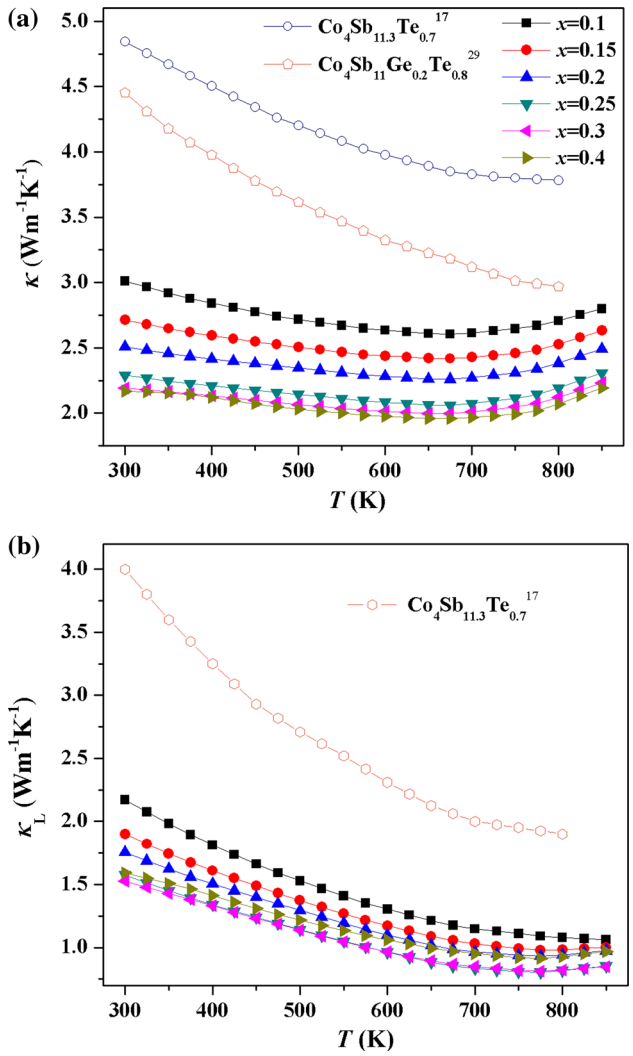

Fig. 6. Temperature dependence of thermal conductivity (a), and lattice thermal conductivity (b) for all samples.

$S_{0.3}Co_4Sb_{11.2}Te_{0.8}$ sample is caused by the increasing tellurium content (as shown in Table I) compared to $S_{0.1}Co_4Sb_{11.2}Te_{0.8}$ sample. Similar results can also be found in the Te-doped skutterudites.[17,29]

Figure 3a shows the BSI of the polished surface of the sample $S_{0.3}Co_4Sb_{11.2}Te_{0.8}$. It is apparent that the obtained chemical compositions are basically homogeneous. With the elemental distribution maps (Fig. 3b, c, d, and e), it can be found that the elements (Co, Sb, S and Te) were evenly distributed. The atomic percentages of these elements in different areas of $S_{0.3}Co_4Sb_{11.2}Te_{0.8}$ sample are determined, which are listed in Fig. 3f.

The doping efficiency of tellurium and filling efficiency of sulfur are shown in Fig. 4, which calculated the ratio of the actual content to the nominal content of tellurium and sulfur in all samples. Compared to single Te-doping skutterudite,[17,20] S-filling can enhance the doping efficiency of tellurium significantly. The main reason is that the sulfur exists in an electronegative ionic state in skutterudite, and it can promote the doping efficiency of tellurium under the effect of charge compensation. Similar principle and results can also be found in the electropositive guests (such as Yb and Sr) filled and group IVA atoms (such as Sn and Ge) doped skutterudites,[26–28] and also the Ge/Sn-Te co-doped skutterudites.[11,12,19] In addition, it should be noted that charge compensation such as substituting a small amount of Te at the Sb site is a necessary condition for sulfur filled $CoSb_3$,[20] which can also enhance the filling fraction of the sulfur. The doping efficiency of tellurium is enhanced with incremental sulfur content, which makes the actual composition of samples closer to the nominal composition. The impurity phases decrease accordingly. This phenomenon is consistent with the XRD test results. Tellurium has the much larger radius than those of antimony, so increasing the tellurium content will lead to larger lattice parameters,[30] as shown in Table I. When the filling fraction of sulfur reaches $x = 0.4$, the content of tellurium is reduced

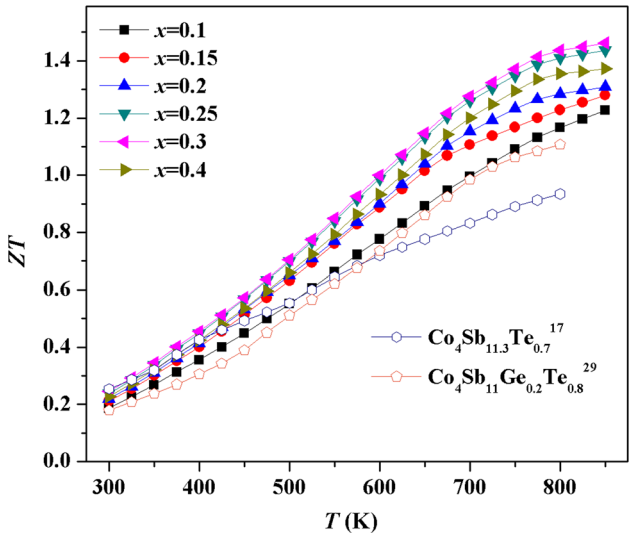

Fig. 7. Dimensionless figure of merit *ZT* for all samples.

compared with $x = 0.3$, indicating that the doping of tellurium reaches the solubility limit at $x = 0.3$ in this work, and further increasing sulfur content leads to the lattice shrinkage of $S_{0.4}Co_4Sb_{11.2}Te_{0.8}$ sample (The electronegative filler sulfur attracts the neighboring antimony atoms, which leads to lattice shrinkage[20]).

Figure 5 indicates the electrical transport properties of $S_xCo_4Sb_{11.2}Te_{0.8}$ samples with temperature and filling content. As shown in Fig. 5a, the electrical conductivity of $S_xCo_4Sb_{11.2}Te_{0.8}$ compounds decreases with the increasing filling fraction of sulfur. This is mainly because that the electronegative guest sulfur attracts two electrons, reducing the carrier concentration of *n*-type skutterudite materials.[20] For that reason, the electrical conductivities of all the $S_xCo_4Sb_{11.2}Te_{0.8}$ samples are decreased in comparison with those of the single Te-doping skutterudite[17] and Ge-Te co-doping skutterudite.[29] The negative Seebeck coefficient as shown in Fig. 5b indicates that electrons are the major carriers in the obtained samples. The absolute values of the Seebeck coefficient of all samples increase with increasing S-filling fraction between 300 K and 850 K. And the Seebeck coefficient of $S_{0.4}Co_4Sb_{11.2}Te_{0.8}$ compound attains a maximum value of $-222\ \mu VK^{-1}$ at 850 K.

The temperature-dependent thermal conductivity and lattice thermal conductivity of all the samples are shown in Fig. 6a and b respectively. As shown in Fig. 6a, the thermal conductivity of all samples first decreased (300–700 K) then increased in the high-temperature range (700–850 K), this is mainly attributed to the bipolar diffusion effect.[31] For comparison, the thermal conductivity of single Te-doped[17] and Ge-Te co-doped[29] samples are also plotted. The thermal conductivity for $S_xCo_4Sb_{11.2}Te_{0.8}$ ranges from 3.1 $Wm^{-1}K^{-1}$ ($x = 0.1$) to 2.2 $Wm\text{-}K^{-1}$ ($x = 0.4$) at 300 K, and from 2.7 $Wm^{-1}K^{-1}$ ($x = 0.1$) to 2.1 $Wm^{-1}K^{-1}$ ($x = 0.4$) at 800 K. All these values are much lower than those of Te single-doped and Ge-Te co-doped samples at the same temperatures.[17,29] As shown in Fig. 6b, the lattice thermal conductivity of $S_{0.3}Co_4Sb_{11.2}Te_{0.8}$ at 300 K is 1.52 $Wm^{-1}K^{-1}$, 54% lower than that of single Te-doped samples.[17] The lattice thermal conductivity of $S_{0.3}Co_4Sb_{11.2}Te_{0.8}$ sample attains a minimum value of 0.81 $Wm^{-1}K^{-1}$ at 775 K. It is believed that the low lattice thermal conductivity in this study mainly originates from high doping efficiency of tellurium and filling efficiency of sulfur.

On the basis of Seebeck coefficient, electrical conductivity and thermal conductivity measurements, the figures of the merit *ZT* are calculated, as shown in Fig. 7. The highest value of $ZT = 1.5$ is obtained for $S_{0.3}Co_4Sb_{11.2}Te_{0.8}$ sample at 850 K in contrast with ~ 0.93 for $Co_4Sb_{11.4}Te_{0.6}$ sample[17] at 800 K and ~ 1.1 for $Co_4Sb_{11}Ge_{0.2}Te_{0.8}$ sample[29] at 800 K. Te-doping and S-filling can significantly enhance the thermoelectric properties of skutterudite via reducing the thermal conductivity.

CONCLUSIONS

In this study, *n*-type $S_xCo_4Sb_{11.2}Te_{0.8}$ samples are synthesized with the solid state reaction and spark plasma sintering. The filling effects on the thermoelectric properties are investigated systematically. The obtained results demonstrate that the thermal conductivity of $S_xCo_4Sb_{11.2}Te_{0.8}$ skutterudite is reduced by optimizing the sulfur filling fraction. S-filling can enhance the doping efficiency of tellurium significantly, which is attributed to the charge compensation between electronegative guest sulfur and dopant tellurium. The thermoelectric properties of $S_xCo_4Sb_{11.2}Te_{0.8}$ skutterudite have been significantly enhanced because of low thermal conductivity. Moreover, the $x = 0.3$ sample has the lowest lattice thermal conductivity and the highest *ZT* (1.5, 850 K) over the entire temperature range. Better performance of the electronegative-guest filled skutterudites can be expected by continuing effort to optimize its doping and filling fractions.

ACKNOWLEDGEMENTS

This work was supported by the National Natural Science Foundation of China (Nos. 51772231 and 11572050), the National Basic Research Program of China (No. 2013CB632505), the International S&T Cooperation Program of China (2014DFA63070), and the Fundamental Research Funds for the Central Universities (No. 2016IB001). Besides, H. T. Wang is grateful to C. H. Shen and M. J. Yang for their help with XRD and EPMA in Materials Research and Test Center of WUT.

REFERENCES

1. T.M. Tritt and M.A. Subramanian, *MRS Bull.* 31, 188 (2006).
2. L.E. Bell, *Science* 321, 1457 (2008).
3. A. Patyk, *Appl. Energy* 102, 1448 (2013).

4. T.M. Tritt, *Ann. Rev. Mater. Res.* 41, 433 (2011).
5. K.T. Wojciechowski, *Mater. Res. Bull.* 37, 2023 (2002).
6. F.J. DiSalvo, *Science* 285, 703 (1999).
7. H. Li, X.F. Tang, Q.J. Zhang, and C. Uher, *Appl. Phys. Lett.* 94, 102114 (2009).
8. Y. Lan, A.J. Minnich, G. Chen, and Z. Ren, *Adv. Funct. Mater.* 20, 357 (2010).
9. G. Chen, M.S. Dresselhaus, G. Dresselhaus, J.P. Fleurial, and T. Caillat, *Int. Mater. Rev.* 48, 45 (2013).
10. I.H. Kim and S.C. Ur, *Met. Mater. Int.* 23, 53 (2007).
11. W.S. Liu, B.P. Zhang, L.D. Zhao, and J.F. Li, *Chem. Mater.* 20, 7526 (2008).
12. X.L. Su, H. Li, Y.G. Yan, G.Y. Wang, H. Chi, X.Y. Zhou, X.F. Tang, Q.J. Zhang, and C. Uher, *Acta Mater.* 60, 3536 (2012).
13. P. Qiu, X. Shi, X. Chen, X. Huang, R. Liu, and L. Chen, *J. Alloy. Compd.* 509, 1101 (2011).
14. X.Y. Li, L.D. Chen, J.F. Fan, W.B. Zhang, T. Kawahara, and T. Hirai, *J. Appl. Phys.* 98, 083702 (2005).
15. S. Hui, M.D. Nielsen, M.R. Homer, D.L. Medlin, J. Tobola, J.R. Salvador, J.P. Heremans, K.P. Pipe, and C. Uher, *J. Appl. Phys.* 115, 103704 (2014).
16. M.J. Kim and I.H. Kim, *Met. Mater. Int.* 16, 459 (2010).
17. B. Duan, P.C. Zhai, L.S. Liu, Q.J. Zhang, and X.F. Ruan, *J. Mater. Sci.: Mater. Electron.* 23, 1817 (2012).
18. B.C. Sales, D. Mandrus, and R.K. Williams, *Science* 273, 1725 (1996).
19. B.R. Ortiz, C.M. Crawford, R.W. McKinney, P.A. Parilla, and E.S. Toberer, *J. Mater. Chem. A* 4, 8444 (2016).
20. B. Duan, J. Yang, J.R. Salvador, Y. He, B. Zhao, S.Y. Wang, P. Wei, F.S. Ohuchi, W.Q. Zhang, and R.P. Hermann, *Energy Environ. Sci.* 9, 2090 (2016).
21. S.M. Said, M.B.A. Bashir, M.F.M. Sabri, Y. Miyazaki, D.A.A. Shnawah, A.S. Hakeem, M. Shimada, A.I. Bakare, N.N.N. Ghazali, and M.H. Elsheikh, *Metall. Mater. Trans. A* 48, 3073 (2017).
22. V.L. Kuznetsov, L.A. Kuznetsova, and D.M. Rowe, *J. Phys. Condens. Mat.* 15, 5035 (2003).
23. X.F. Tang, Q.J. Zhang, L.D. Chen, T. Goto, and T. Hirai, *J. Appl. Phys.* 97, 093712 (2005).
24. X.D. Li, B. Xu, L. Zhang, F.F. Duan, X.L. Yan, J.Q. Yang, and Y.J. Tian, *J. Alloy. Compd.* 615, 177 (2014).
25. X. Shi, H. Kong, C.P. Li, C. Uher, J. Yang, J.R. Salvador, H. Wang, L. Chen, and W. Zhang, *Appl. Phys. Lett.* 92, 182101 (2008).
26. G.A. Lamberton, R.H. Tedstrom, T.M. Tritt, and G.S. Nolas, *J. Appl. Phys.* 97, 113715 (2005).
27. N.R. Dilley, E.D. Bauer, M.B. Maple, and B.C. Sales, *J. Appl. Phys.* 88, 1948 (2000).
28. X.Y. Zhao, X.Y. Li, L.D. Chen, Y.Z. Pei, S.Q. Bai, X. Shi, and T. Goto, *Jpn. J. Appl. Phys.* 47, 7470 (2008).
29. B. Duan, P.C. Zhai, L.S. Liu, and Q.J. Zhang, *J. Electron. Mater.* 40, 932 (2010).
30. X.L. Su, H. Li, G.Y. Wang, H. Chi, X.Y. Zhou, X.F. Tang, Q.J. Zhang, and C. Uher, *Chem. Mater.* 23, 2948 (2011).
31. W.S. Liu, B.P. Zhang, J.F. Li, H.L. Zhang, and L.D. Zhao, *J. Appl. Phys.* 102, 103717 (2007).